Journal of Power Sources 182 (2008) 265–269

Contents lists available at ScienceDirect

Journal of Power Sources

journal homepage: www.elsevier.com/locate/jpowsour

Short communication

An improved model for predicting electrical contact resistance between bipolar plate and gas diffusion layer in proton exchange membrane fuel cells

Zhiliang Wu [a], Yuanyuan Zhou [b], Guosong Lin [b], Shuxin Wang [a], S. Jack Hu [b,*]

[a] School of Mechanical Engineering, Tianjin University, Tianjin 300072, PR China
[b] Department of Mechanical Engineering, The University of Michigan, Ann Arbor, MI 48109-2125, USA

ARTICLE INFO

Article history:
Received 14 December 2007
Received in revised form 4 March 2008
Accepted 4 March 2008
Available online 25 March 2008

Keywords:
PEM fuel cell
Electrical contact resistance
Multiple regression

ABSTRACT

Electrical contact resistance between bipolar plates (BPPs) and gas diffusion layers (GDLs) in PEM fuel cells has attracted much attention since it is one significant part of the total contact resistance which plays an important role in fuel cell performance. This paper extends a previous model by Zhou et al. [Y. Zhou, G. Lin, A.J. Shih, S.J. Hu, J. Power Sources 163 (2007) 777–783] on the prediction of electrical contact resistance within PEM fuel cells. The original microscale numerical model was based on the Hertz solution for individual elastic contacts, assuming that contact bodies, GDL carbon fibers and BPP asperities are isotropic elastic half-spaces. The new model features a more practical contact by taking into account the bending behavior of carbon fibers as well as their anisotropic properties. The microscale single contact process is solved numerically using the finite element method (FEM). The relationship between the contact pressure and the electrical resistance at the GDL/BPP interface is derived by multiple regression models. Comparisons of the original model by Zhou et al. and the new model with experimental data show that the original model slightly overestimates the electrical contact resistance, whereas a better agreement with experimental data is observed using the new model.

1. Introduction

Interest has been growing in proton exchange membrane (PEM) fuel cells due to their unique characteristics of low operation temperature, low emission and quick startup. However, various irreversible losses existing in an operating PEM fuel cell affect its performance and reduce its efficiency. Ohmic loss is one of the main losses in normal fuel cell operation. The contribution from the contact resistance to the ohmic loss has been reported to be approximately equal to that from the proton conduction resistance in the membrane [2].

The contact resistance in a PEM fuel cell is dominated by the contact resistance at the interface between the bipolar plate (BPP) and the gas diffusion layer (GDL) [2–4]. A schematic of the contact at the interface is shown in Fig. 1. The resistance is closely related to the material properties, surface topology and treatment, assembly pressure and cell operation conditions. Various work has been done on the measurement [2–7], prediction [1,4,8] and improvements [9,10] of the electrical contact resistance.

This paper extends the work by Zhou et al. [1] by improving the accuracy of electrical contact resistance prediction in a PEM fuel cell. The improvement is achieved by taking into account the bending behavior of the carbon fibers in the GDL and their anisotropic properties. The single contact between a GDL carbon fiber and a BPP asperity is modeled by the finite element method (FEM). Regression models for the contact force and the contact area are then developed based on Latin hypercube sampling (LHS) taking fiber length, contact location and compression displacement as inputs. The overall contact resistance is calculated by numerical simulations assuming the input variables follow certain random distributions. The numerical results demonstrate a more reasonable agreement with the experimental data.

The remainder of the paper is organized as follows. Section 2 reviews the previous contact resistance model by Zhou et al. [1]. Section 3 elaborates on the improvements over the original model and discusses the multiple regression models for the contact force and the contact area. Section 4 presents the results and discussions. Section 5 draws the conclusions.

* Corresponding author. Tel.: +1 734 615 4315; fax: +1 734 647 7303.
E-mail address: jackhu@umich.edu (S.J. Hu).

0378-7753/$ – see front matter © 2008 Elsevier B.V. All rights reserved.
doi:10.1016/j.jpowsour.2008.03.044

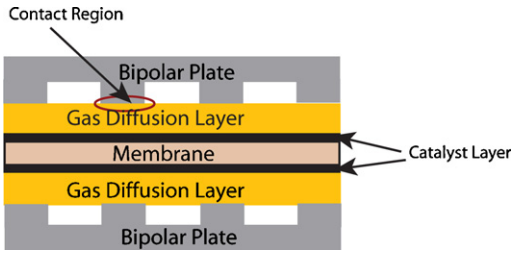

Fig. 1. Schematic structure of a PEM fuel cell [1].

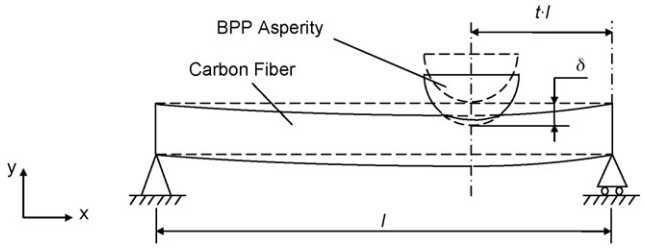

Fig. 3. Schematic of the microscale contact between a BPP asperity and a carbon fiber.

2. Review of microscale contact resistance model

In this paper, numerical models of the BPP surface profile and the GDL structure are generated using the same methods as in Zhou et al. [1]. The BPP surface is built according to Greenwood and Williamson's model [11]. The surface profile follows a Gaussian distribution in summit heights and the asperities are spherical in shape with an identical radius of curvature. The spatial distribution of summits is also assumed to obey a uniform distribution. The BPP sample used in the experiment is a grade FU 4369 graphite plate from PEM Technology Inc. The surface profile is numerically generated using parameters extracted from the experimental data recorded by a profilometer with a lateral resolution of 0.5 μm. Several scans in different sections of the BPP surface were conducted to obtain the roughness parameters for the entire surface.

The GDL material is modeled based on scanning electron micrograph (SEM) images of a Toray TGP-H-30 PAN-based carbon fiber paper. The SEM images indicate that the carbon paper exhibits a structure of multiple carbon fiber layers with binders in between. Cylindrical fibers in the structure are randomly distributed in length and orientation with a diameter of 7 μm. The binder thickness between two adjacent fiber layers is 4 μm. A critical parameter of the generated GDL structure is the total carbon fiber length in a unit area, which is estimated as 57 mm mm^{-2} from the SEM measurements. The generated surfaces are shown in Fig. 2.

The single micro-contact response was calculated using Hertz theory [12] in the work by Zhou et al. [1]. In the present model, the contact force and the contact area are analyzed by the FEM under the same basic assumptions of no interactions between the BPP asperities, no bulk deformation in the BPP and contacts being entirely elastic. The contact area is also assumed to be planar and circular. The new elements in the new model are the bending behavior of carbon fibers and their anisotropic material properties. The constriction resistance is calculated according to Holm's theory [13]. The overall contact resistance at the interface is obtained by considering all contact spots as resistances in parallel and the clamping force is equivalent to the sum of forces on the contact spots.

3. Microscale contact model with fiber bending and anisotropic behavior

3.1. FEM model

In a PEM fuel cell stack, asperities on the BPP come into direct contact with carbon fibers due to the assembly pressure. The contact resistance between the BBP and the GDL can be viewed as an overall effect of the contributions from individual contacts. A microscale contact is modeled as a contact between a spherical asperity with a radius of 3.67 μm and a cylindrical fiber with a cross-section diameter of 7 μm. With the assumption of layered structure of the GDL material, fibers at the upper layer are supported by those at the lower layer. The contact process is then reduced into a beam bending problem as shown schematically in Fig. 3. The carbon fibers in contact are modeled as simply supported beams. The support locations are determined by calculating the contact locations between the upper and lower layers. The effective fiber length between any two supports varies since carbon fibers are of random positions and orientations.

An elastic finite element method is used to solve the sphere–beam contact problem. It is assumed that the BPP asperities are in frictionless contacts with the carbon fibers. The material properties of the BPP and carbon fibers in the diffusion medium are presented in Table 1. The subscriptions L and T indicate the longitudinal and transverse directions of the carbon fibers, respectively. The bending problem is numerically solved using the commercial FEM package ANSYS. Eight-node brick elements (SOLID 45) are used to model the elastic structures. The BPP asperity surface is defined as the target surface and modeled with elements TARGE 170, while the carbon fiber surface is defined as the contact surface and modeled with elements CONTA 173. The mesh consists

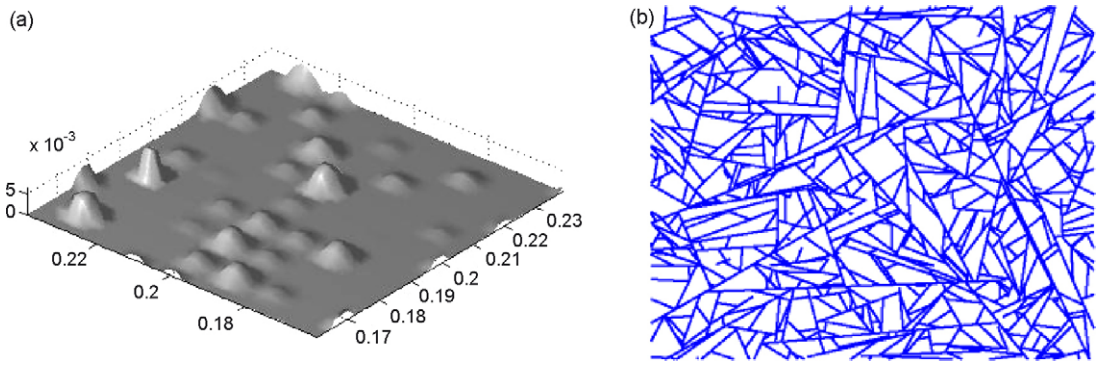

Fig. 2. (a) Generated BPP surface profile and (b) simulated GDL structure [1].

Table 1
Material properties of carbon fibers and the BPP

Materials	E_L (GPa)	E_T (GPa)	ν_{LT}	ν_{TT}	G_{LT} (GPa)	G_{TT} (GPa)
Carbon fibers	230[a]	3.20[b]	0.256[c]	0.300[c]	27.3[c]	3.08[c]
BPP	10[b]		0.26[b]			

[a] Reported by Ref. [14].
[b] Reported by Ref. [1].
[c] Reported by Ref. [15].

Table 2
Different contact models

B	A	
	No	Yes
No	I	II
Yes	III	IV

of a total of about 100,000 nodes (depending on the fiber length). An ANSYS Parametric Design Language (APDL) program is developed to calculate the contact force and the contact area for various contact situations represented by a combination of the effective fiber length, the contact location, and the compression as input variables.

Four contact models as indicated in Table 2 are built to evaluate the effects of bending and anisotropic behaviors of the carbon fibers. In the table, "A" denotes the anisotropic material property and "B" represents the bending behavior. Fiber bending is not included in situation I and III where the lower section of the carbon fiber between the two supporting points is completely fixed as the boundary condition.

3.2. Multiple regression models for microscale contact

When the assembly force is applied on a PEM fuel cell, there might be as many as hundreds or even thousands of contact spots per square millimeter at the BPP/GDL interface. It is impractical to calculate the contact force and the contact area for every contact spot using the FEM. Therefore, an analytical approximation for the contact force–contact area relationship is desired. In this section, multiple regression models for the contact force and the contact area are developed for the four contact models listed in Table 2 using computational experiments.

Latin hypercube sampling (LHS), one of the most commonly employed space filling designs for deterministic computer simulations [16], is used to select a suitable set of tests for finite element analysis. LHS was originally proposed by Mckay et al. [17] as an alternative to simple random sampling and with a more accurate estimation of the mean value. Another outstanding feature of LHS is that it is not restricted to sample sizes that are certain multiples or powers of the number of design variables. In our study a LHS of size $n = 19$ with three design variables are generated for the sphere–beam contact problem. The sample size is assigned as a compromise of computational cost and accuracy. The design variables are the fiber length (l) with a normal distribution, the contact location (t) with a uniform distribution, and the compression (δ) with a normal distribution. The sampling procedure completes with the responses, the contact force (F) and the contact area (A), being calculated using the FEM for each of the 19 input vectors. Sampling for the situations without bending is conducted in a similar way with the compression as the only design variable.

The relationships between the contact force/contact area and the predictor variables are observed to be linear in the log domain by examination of the residual plots. Therefore, multiple linear regression models are used to estimate the relationships with a log transformation on the variables. The method of least squares is used to estimate the regression coefficients. Testing hypotheses on the individual regression coefficients are conducted by evaluating the t-ratio to obtain a more effective regression model [18]. The following models are obtained with respect to the four situations shown in Table 2:

Model I: contacts without bending and carbon fibers as isotropic materials:

$$\log F_i' = 2.01 + 1.61 \log \delta \quad (1)$$

$$\log A_i' = 2.10 + 1.01 \log \delta \quad (2)$$

Model II: contacts with bending and carbon fibers as isotropic materials:

$$\log F_i = 4.26 - 1.65 \log l - 0.814 \log t + 0.995 \log \delta \quad (3)$$

$$\log A_i = 3.57 - 1.04 \log l - 0.510 \log t + 0.557 \log \delta \quad (4)$$

Model III: contacts without bending and carbon fibers as anisotropic materials:

$$\log F_a' = 2.10 + 1.63 \log \delta \quad (5)$$

$$\log A_a' = 1.96 + 0.984 \log \delta \quad (6)$$

Model IV: contacts with bending and carbon fibers as anisotropic materials:

$$\log F_a = 3.52 - 0.721 \log l - 0.258 \log t + 1.17 \log \delta \quad (7)$$

$$\log A_a = 2.97 - 0.513 \log l - 0.169 \log t + 0.893 \log \delta \quad (8)$$

The regression models for contacts without bending are significant ($p < 0.0005$) and with an adjusted R^2 of over 0.99 and those for contact with bending are significant ($p < 0.0005$) and with an adjusted R^2 of over 0.95, indicating most of the variation in the contact responses can be explained by the variables in the equations. Thus, the contact force and contact area for the micro-contact can be determined once the parameters in the regression models are decided by the GDL structure and the BPP surface profile. The total contact force is obtained by summing up individual microscale contact forces and the contact resistance at the BPP/GDL interface is the parallel resistance of the micro-contact spots.

4. Results and discussion

The contact resistance at an interface is usually believed to be a negative power function of the applied load [11,13,19]. Fig. 4 displays the log–log relationships of the contact resistance versus assembly pressure by the four regression models and the previous result by Zhou et al. [1]. All of the five lines in the figure have a similar slope, which confirms that the contact resistance at the BPP/GDL interface decreases with a certain power function of the clamping pressure. As observed from the log–log curves, the contact resistance in the PEM fuel cell reduces as a result of bending behavior of carbon fibers but increases due to their anisotropic properties. Histograms of the

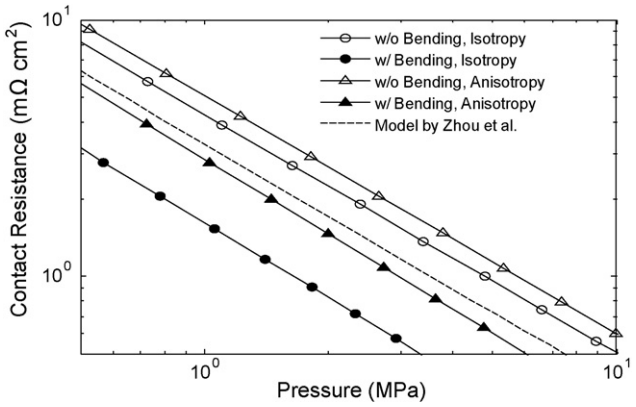

Fig. 4. Log–log plot of the contact resistance vs. assembly pressure relationship by the regression models.

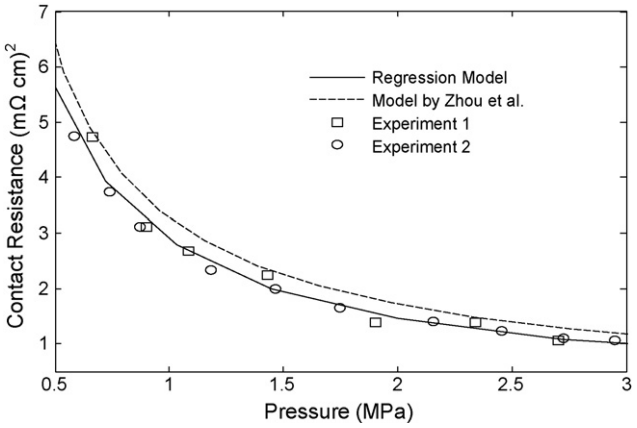

Fig. 6. Comparison between the new model and the original model.

number of contacts and the total contact resistance are plotted in Fig. 5 for the four contact situations when the assembly pressure is 1 MPa. Comparison for both isotropic and anisotropic carbon fibers indicates that under the same assembly pressure, more micro-contacts occur at the interface with a smaller average micro-contact area for the models with bending than without. According to Holm [13], the resistance of individual contact spots is inversely proportional to the square root of the contact area. The overall contact resistance is inversely proportional to the number of contacts that are treated as resistances in parallel. The increase in the number of micro-contacts tends to reduce the overall contact resistance, but the reduction in the micro-contact area has an opposite effect. As illustrated in Fig. 5, the effect of the increase in the number of contacts overweighs that of the reduction in the average micro-contact area. That is, the contact resistance at the interface reduces as a result of the bending behavior of carbon fibers. For anisotropic carbon fibers, their transverse properties can be as small as a fraction of their axial properties. Compared to isotropic carbon fibers with lower mechanical properties, the anisotropic fibers are less deformed and the contact resistance becomes larger under the same pressure. It might also be noted in Fig. 4 that the result by regression model I is observed to deviate from the estimate by Zhou et al. [1], although both are based on the assumption that the carbon fibers are isotropic and no fiber bending is included during contact. The deviation is believed to be caused by the simplification in the Hertz theory that each contact body is regarded as an elastic half-space [12].

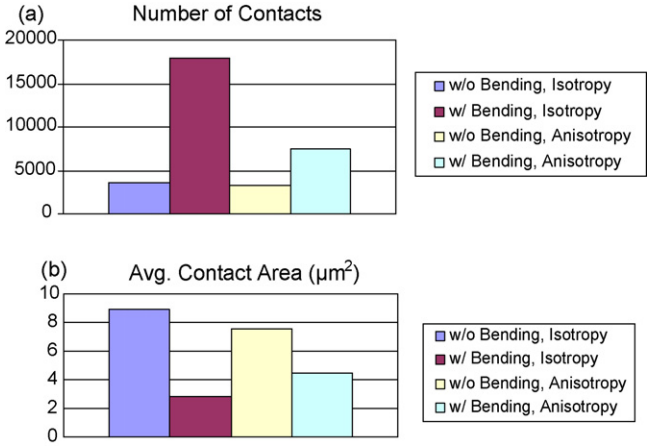

Fig. 5. Comparison of the number of contacts and the average micro-contact area at 1 MPa: (a) number of contacts and (b) average micro-contact area.

An improvement in prediction of the contact resistance versus assembly pressure relationship by regression model IV is illustrated in Fig. 6. It is manifested through comparison with the experimental data that the original model by Zhou et al. [1] slightly overestimates the contact resistance, while a more reasonable prediction is obtained by this new model. The improvement is a combination effect of the fiber bending behavior and the anisotropic material property.

5. Conclusions

This paper improves the microscale contact resistance model proposed by Zhou et al. [1] for the prediction of the electrical contact resistance between the BPP and the GDL in a PEM fuel cell. In this present model, the material anisotropy of GDL carbon fibers and their bending behaviors were included in the modeling of the micro-contact between the BPP asperities and the GDL carbon fibers using the FEM. Multiple regression models and computer experiments were developed to estimate the contact force and the contact area for individual contacts. Results show that under the same assembly pressure, the contact resistance tends to reduce as a result of fiber bending, but increase when the anisotropic behavior is included in the model. A more reasonable estimate of the contact resistance versus pressure relationship was achieved by including the bending and anisotropic behaviors of the carbon fibers in the GDL.

Based on the regression models, a parametric study can be conducted to evaluate the sensitivities of variables that affect the contact resistance between the gas diffusion layer and the bipolar plate in PEM fuel cells. The contact resistance can be reduced by controlling the surface roughness of the bipolar plate and the fiber configuration of the gas diffusion layer, and by selecting materials for the gas diffusion layer and the bipolar plates with properties that are conducive to low contact resistance.

References

[1] Y. Zhou, G. Lin, A.J. Shih, S.J. Hu, J. Power Sources 163 (2007) 777–783.
[2] H.A. Gasteiger, M.F. Mathias, The Workshop on Materials for High Temperature PEM Fuel Cells, The Pennsylvania State University, December 11, 2003.
[3] T. Berning, N. Djilali, J. Power Sources 124 (2003) 440–452.
[4] V. Mishra, F. Yang, R. Pitchumani, J. Fuel Cell Sci. Technol. 1 (2004) 2–9.
[5] F. Barbir, J. Braun, J. Neutzler, J. New Mater. Electrochem. Syst. 2 (1999) 197–200.

[6] W.K. Lee, C.H. Ho, J.W. Van Zee, M. Murthy, J. Power Sources 84 (1999) 45–51.
[7] J. Ihonen, F. Jaouen, G. Lindbergh, G. Sundholm, Electrochim. Acta 46 (2001) 2899–2911.
[8] L. Zhang, Y. Liu, H. Song, S. Wang, Y. Zhou, S.J. Hu, J. Power Sources 162 (2006) 1165–1171.
[9] R.H.J. Blunk, D.J. Lisi, Y.E. Yoo, C.L. Tucker III, AIChE J. 49 (2003) 18–29.
[10] A. Heinzel, F. Mahlendorf, O. Niemzig, C. Kreuz, J. Power Sources 131 (2004) 35–40.
[11] J.A. Greenwood, J.B.P. Williamson, Proc. R. Soc. Lond. A 295 (1966) 300–319.
[12] K.L. Johnson, Contact Mechanics, Cambridge University Press, 1985, pp. 84–106.
[13] R. Holm, Electric Contacts Theory and Application, Springer-Verlag, New York, 1967, pp. 9–16.
[14] Toray Industry Inc., Technical data sheet.
[15] H. Miyagawa, C. Sato, T. Mase, E. Drown, L.T. Drzal, K. Ikegami, Mater. Sci. Eng. A 412 (2005) 88–92.
[16] A.A. Giunta, S.F. Wojtkiewicz Jr., M.S. Eldred, Proceedings of the 41st AIAA Aerospace Sciences Meeting and Exhibit, Reno, NV, 6–9 January, 2003.
[17] M.D. McKay, R.J. Beckman, W.J. Conover, Technometrics 21 (1979) 239–245.
[18] D.C. Montgomery, Design and Analysis of Experiments, fifth ed., John Wiley & Sons, Inc., New York, 2001, pp. 392–421.
[19] R.A. Oniions, J.F. Archard, J. Phys. D: Appl. Phys. 6 (1973) 289–304.